Resonant Microsensors: Fundamentals and State of the Art.

by M.J. Tudor and S.P. Beeby*

Microengineering Centre

ERA Technology

Cleeve Road

Leatherhead

Surrey

KT22 7SA

England

Tel +44 (0) 1372 367000

FAX +44 (0) 1372 367099

*University of Southampton Institute of Transducer Technology (USITT)

University of Southampton

Southampton

Hampshire

England

Tel: +44 (0)1703 593545

Fax: +44 (0)1703 592738

(Received June 13th, 1995)

Resonant Microsensors: Fundamentals and State of the Art

Abstract

Resonant sensors offer a high performance solution to many sensing applications. This paper presents a review of resonant microsensors based upon resonant structures fabricated in silicon, quartz and gallium arsenside. The methods of coupling the resonator to the measurand are discussed and example sensors for pressure, acceleration and rotation sensing applications are introduced. Important design considerations such as resonator geometry, the Q-factor, nonlinear behaviour, power consumption and packaging are analysed. Lastly the relative merits of silicon, quartz and GaAs as a resonator material are reviewed.

Keywords

Resonant sensors, Silicon, Quartz, Gallium Arsenide, Q-factor.

1 : Introduction

Resonant sensors offer high accuracy (0.01%FS), low drift (ppmFS/year) and high resolution. However traditional resonant sensors have required painstaking machining of the metal resonator and careful hand assembly of the complete sensor. Their excellent performance characteristics have justified their use in applications such as aircraft engine management systems and high accuracy

pressure controllers, but the high cost of traditional resonant sensors has limited their widespread application.

Micromachined resonant sensors or resonant microsensors are fabricated in batches on a silicon, quartz or gallium arsenide wafers. They are therefore significantly cheaper and smaller than traditional resonant sensors with a performance which should be comparable to, if not better than, that of traditional devices. It is therefore probable that resonant microsensors will be more widely applied than their traditional ancestors.

This paper reviews the fundamental operating principles of resonant microsensors and the current state of the art. It is a complementary paper to other recent review articles.[1,2] Examples are given of the most important types of resonant microsensors, these being: pressure sensors, accelerometers and gyroscopes. Then, the design rules for resonant sensors are outlined followed by a discussion of the materials and fabrication techniques which can be used in the manufacture of microresonant devices. Finally the most important resonator cross sensitivities are outlined.

2 : Basic Principles of Resonant Sensors

Figure 1 shows a block diagram of a typical resonant sensor. The heart of the resonant sensor is a mechanical structure vibrating at its resonant frequency. The vibrations are excited by using some form of drive technique (eg electrostatic)

and sensed by some form of detection technique (eg piezoresistive). Drive and detection can be separate (two-port configuration) or combined (one-port configuration).[3] Electronic circuitry, usually either a simple amplifier or a phase-locked loop, provides feedback from detection to drive. By this means the resonator is maintained vibrating continuously at its resonant frequency.

The predominant form of resonant microsensor provides a frequency output; that is its mechanical structure's resonant frequency is a function of the measurand. This has been achieved in three ways: by applying a force or stress to the resonator thus changing its stiffness, by altering the mass of the resonator or by changing the shape of the resonator.[1,2] The stiffness effect has been applied in micromachined pressure sensors[4,5,6] and accelerometers.[7,8,9] The added mass effect has been used in the quartz crystal microbalance often used as a thickness monitor in thin film coating systems[10] and the shape effect has been applied to realise a pressure sensor.[11]

To date the stiffness and added mass effects are the most commonly applied and are illustrated in Figs. 2 and 3. Figure 2 shows the change in frequency of modes 1 to 3 of a clamped-clamped beam in response to applied axial loads. The frequency shift plotted is in relation to the unstressed frequency for each mode. The figure shows the effects of both compressive and tensile loads, the applied load being plotted with respect to the maximum compressive stress the beam can withstand before buckling (P/P_b).[12]

A second, and less well developed, form of resonant microsensor relies on the effect of the Corriolis force on a resonating structure. Such an effect has been applied in a resonant micro-gyroscope[13,14] as well as in conventional flow sensors.[15] Figure 4 shows the relationship between the Corriolis force and the resonant sensor's output, which is the amplitude of an induced parasitic vibration.

A third form of resonant sensor relies on the damping effect of the surrounding fluid on the resonator's Quality factor (Q-factor). The Q-factor is a figure of merit describing a resonance (see section 4.4). A resonant sensor based upon the Q-factor can act as a viscometer[16], pressure sensor[17] or vacuum sensor.[18] The use of microresonators will be limited in such applications due to their small dimensions and thus fragility. Figure 5 shows the relationship, between a bridge style resonator's Q-factor and the viscosity of the surrounding fluid.

3 : Examples of Resonant Microsensors

In the following sections the operating principles of the main type of resonant microsensor are briefly described. More details are given in reference 1.

3.1 Absolute and differential pressure

Micromachined resonant pressure sensors based on the axial stiffness effect are commercially available. In such devices the resonator is normally isolated from the pressurised medium to avoid density cross sensitivity as well as

the influence of other disturbing loads. The resonator is often integrated in, or mounted on, one surface of a diaphragm and maintained in a vacuum to ensure a high Q-factor. The other surface of the diaphragm is exposed to the pressure medium. A pressure difference across the diaphragm therefore causes it to bend thus stressing the resonator and so altering its resonant frequency. Figure 6 shows an early example, now commercially available.[4] A differential pressure sensor, now also in production, is described in ref. 19.

3.2 Acceleration

Micromachined accelerometers have also been demonstrated based on the stiffness effect but are not yet commercially available. Silicon resonant accelerometers usually consist of an inertial mass supported by one, two or four resonators.[7,20] Acceleration of the device in its sensitive plane produces an inertial force on the resonators thus altering their frequency. In the multiple resonator version a differential approach can be employed. Acceleration becomes a function of the difference in frequency between the resonators and this reduces sensitivity to cross axis accelerations and temperature. Figure 7 shows an example which uses a single, double ended tuning fork resonator.[7]

3.3 Rotation rate

Finally, the Corriolis effect based gyroscope is an important resonant microsensor.[21] The majority of microgyros to date have been produced in quartz. Such devices consist of a resonator such as a tuning fork vibrating in a high Q-factor mode. Rotation of the tuning fork about its axis induces, by means of the Corriolis force, a second parasitic vibration perpendicular to the driven mode of vibration. The amplitude of the parasitic vibration is proportional to the rotation rate of the resonator.

4 : Design Considerations

4.1 Resonator geometry and mode of vibration

The fundamental resonator geometries are cantilever beams, bridges and diaphragms. The bridge design, consisting of a single beam fixed at both ends to the surrounding structure, is the most commonly used as it is simple to fabricate and operate. It may vibrate in torsional or flexural modes. More complex resonator geometries offering improved performance characteristics include tuning forks (TF), double ended tuning forks (DETF), triple beam double ended tuning forks (TB) and even quadruple beam double ended tuning forks (QDB).[1,22,23] Such resonators offer dynamically balanced modes of vibration in which the sum of the forces and moments at the supports due to the tine motion is

close to zero. This reduces vibration sensitivity and, for vacuum encapsulated single crystal resonators, usually results in a high Q-factor and therefore improved sensor resolution.

Balanced modes also offer improved long term drift because the surrounding structure does not participate in the resonator's vibrations and so its influence is minimised. Other high Q-factor resonator designs include various plate structures supported at the nodes operating in torsional modes.[4,24] The resonator in ref. 24 also incorporates an isolating mass structure that further improves the Q-factor of the device. Table 1 gives some examples of resonators which have been fabricated to date.

4.2 Excitation/detection techniques

Many techniques have been investigated for the excitation and detection of resonator vibrations. These are described in detail in paper four[3] of this special issue and so are not mentioned further here.

4.3 Importance of nonlinear behaviour

For a resonating structure the frequency is a function of the square of the amplitude of vibration.[31] This results from the nonlinear relationship between a resonator's restoring force and its amplitude of vibration. The sign and magnitude of the nonlinearity depend on the resonator geometry being particularly influenced

by the support conditions. However, provided the vibration amplitude is kept small compared with the radius of gyration of the beam cross section, such effects are negligible.[32] However at large amplitudes a change in amplitude due to for example, a drift in amplifier gain, may cause a significant frequency change indistinguishable from a measurand change. Thus if the device is operated at large amplitudes automatic gain control may be used to reduce this effect.[4,33] Hysteresis effects[34] occur in the resonance curve at even larger amplitudes and therefore resonant sensors are never operated in this regime.

4.4 Importance of Q-factor

The Q-factor of the mode of vibration is of great importance in resonator design. It must be high enough so that, should the phase of the maintaining electronics drift, the resulting frequency change will be negligible compared with the required overall accuracy and drift requirements. In addition the Q factor is a measure of the sharpness of the resonance curve and thus determines the sensor's resolution. Finally the Q factor is inversely proportional to the power consumption of the resonator and thus a high Q-factor is desirable in battery or low power applications.

The Q-factor is limited by three types of damping mechanism. The most significant mechanism is due to the interaction of the resonator with its surrounding fluid. This can be avoided by operating the resonator in a vacuum

(see section 4.7). The energy coupled from the resonator through its supports to its surroundings represents the second most important mechanism and this can be minimised by the employing various resonator designs as discussed in section 4.1. The third damping mechanism results from energy dissipated internally within the resonator material.

The Q-factor must not be too high since the amplitude at which hysteresis in the resonance curve occurs, due to non linear behaviour, is inversely proportional to $Q^{1/2}$.[34] Thus with a very high Q-factor the vibration amplitude may need to be kept very low.

4.5 Influence of maintaining electronics

Maintaining electronics consist either of a simple feedback amplifier or a phase-locked loop circuit. In general the amplifier aims to keep a fixed relationship between the detected resonator amplitude or velocity and the resonator driving force. At resonance the driving force is in phase with the resonator velocity and leads its displacement by $\pi/2$ radians.[35] The bandwidth of the resonance curve is determined by the 45^o phase shift points either side of resonance. Thus the bandwidth of the resonance in Hz corresponds to 90^o of phase shift. So for a typical Q of 10^5 at 100kHz, the bandwidth of 1Hz corresponds to 90^o of phase shift. By estimating the expected phase drift of the electronics, one can hence arrive at the expected frequency drift of the sensor from this source. It

can be seen, from the above example that a higher Q reduces sensitivity to electronics drift.

4.6 Power consumption

The power consumption in a micromachined resonator is extremely low. It is equated to the energy lost per cycle, E_L which can be evaluated from:

$$E_L = \frac{2\pi}{Q} E_s$$

Where E_S denotes the stored energy which is equal to the kinetic energy as the resonator passes through its centre of motion. The maximum kinetic energy for a clamped clamped beam is given by [36] :

$$E_S = 6\pi^2 lt\rho w f^2 y_m^2$$

where ρ is the density, t is the beam thickness, w is the beam width, l is the beam length, f is the resonant frequency and y_m is the amplitude. Inserting typical values for a silicon beam resonator of: ρ = 2330 kg m^{-3}, t = 5x10^{-6}m, w = 40x10^{-6}m, l = 600x10^{-6}m and f = 10^5 Hz results in E_S equal to 1.66 x 10^{-10} J for 1 μm amplitude of vibration.

Assuming a Q of 10^5 gives a power consumption of only 10.4 nW, this representing the actual power dissipated by mechanical damping effects on the resonator. The electrical drive energy will be greater than this since no drive mechanism possesses 100% efficiency. In addition, the power consumed by the maintaining electronics and vibration detection mechanism must be considered.

4.7 Encapsulation and packaging

Resonant sensors generally require a reference vacuum around the resonator. This has been accomplished at wafer level using a sacrificial layer technique.[19] Alternatively the resonator may be held in a hermetic can.[37] The sacrificial layer technique is more elegant since the resonators are sealed within a vacuum whilst still in the clean room. This ensures maximum cleanliness and minimises the probability of drift. However the vacuum cavity formed by a sacrificial layer technique has a minute volume and thus must be completely hermetic if a good vacuum is to be maintained throughout the sensor's lifetime.

The chip containing the resonant sensor can be packaged in similar ways to piezoresistive sensors, i.e. using standard materials and headers derived from the integrated circuit packaging industry. If packaging stress is a problem an isolating intermediate layer made of pyrex or silicon[38] can be used. Decoupling zones can be formed within this isolating layer[39] or directly on the sensor chip.[40]

5: Material and Fabrication Issues

Single crystal materials such as silicon, quartz and gallium arsenide exhibit low acoustic attenuation and hence possess very high intrinsic Q factors.[41] They are available in wafer form to high purity and with few dislocations, which leads to low resonator drift rates.

The development of single-crystal silicon for integrated circuit fabrication has led to its use in micromachined resonator sensors.[42] Silicon has a strength comparable to that of steel, is elastic up to fracture resulting in minimal hysteresis and has an acceptable temperature coefficient of flexural resonant frequency of around -29 ppm/^{o}C.[43] The fabrication technologies used by the semiconductor industry are applicable to micromechanical structures, allowing many resonator designs to be realised in silicon. Unlike quartz, silicon is not piezoelectric and therefore alternative drive and excitation mechanisms need to be incorporated. Silicon is however piezoresistive with a high gauge factor allowing simple detection of resonator vibrations. The use of silicon also offers the attractive possibility of integrating any required circuitry on the sensor chip.

In the case of sensor and electronics integration it is common for the resonator to be fabricated from polysilicon given the compatibility requirements of the fabrication processes. Polysilicon has a granular structure, the material properties being dependent on the crystal orientations of the individual grains and the grain boundaries. The actual properties vary for each thin film according to

prior surface preparation, deposition conditions and post processing steps such as annealing.[44,45] Very fine grained, even amorphous, polysilicon layers are typically used in micromechanical applications such as resonant sensors. Polysilicon is not piezoelectric, so the excitation and detection mechanisms must be incorporated into the structures, the most common being thermal and capacitive. It also exhibits a piezoresistive effect but with a lower gauge factor than the single-crystal form. The stability of polysilicon has been shown to be satisfactory for resonators.[27] However ageing characteristics and Q factors are expected to be degraded when compared with the single-crystal material.

Quartz is available either as amorphous fused quartz (quartz glass) or crystalline quartz, the single-crystal form being used in resonator applications.[46] Crystalline quartz has anisotropic material properties and is piezoelectric, providing a simple means of exciting and detecting resonator vibrations and also allowing the high Q-factor shear modes to be activated. Quartz exhibits superior aging characteristics to silicon and gallium arsenide, and its linear temperature coefficient of frequency is zero for certain modes in certain crystal orientations. The main disadvantages of quartz include the limited machining processes which are available when compared to silicon and the fact that electronics cannot be integrated in quartz. Furthermore the cost of quartz wafers is significantly higher than silicon wafers.

GaAs is the latest material to be considered for microresonator applications.[28] Like quartz it is a piezoelectric material and like silicon it has the potential for integrated circuitry. GaAs has anisotropic material properties and exhibits elastic behaviour up to brittle fracture indicating minimal hysteresis. Its intrinsic Q factor has been reported to be superior to that of silicon,[47] and its time and temperature stability are comparable. Its disadvantages compared to silicon include increased manufacturing costs, less developed processing technologies and higher temperature coefficient of flexural resonant frequency of -48 to -59 ppm/^{o}C[28] and lower strength.

The micromachining of silicon is the most understood of the three materials benefiting from process developments in the IC industry. Micromachining falls into two categories, bulk or surface machining. Bulk micromachining involves the selective etching of silicon from the wafer using wet chemical or dry beam etchants. Resonators can be formed by etching completely through pre-thinned regions of the wafer. Pre-thinned areas may conveniently be formed by etching a diaphragm from the wafer back. The resonator is then formed on the top surface of the diaphragm by protecting those regions where no etching is required that is the resonator itself and its supporting structure.[48]

Resonator based pressure sensors have been fabricated by etching a cavity in the top surface of a diaphragm and bonding a wafer over the cavity. Etching

and polishing of this bonded wafer leaves a thin silicon layer over the cavity from which a resonator can be formed by etching right through to the cavity beneath.[5]

Resonators can be also fabricated using etch stops that render selected regions of the wafer insoluble to the etchant.[4] For example silicon doped with boron concentrations exceeding $4x10^{19}$atoms/cm^3 becomes insoluble to alkaline etchants. This does however cause contraction of the crystal lattice[49] inducing structural stresses and precludes the fabrication of electronic devices in the doped region.

The level of boron concentration can be reduced by employing electro-chemical etch stops,[50] whereby etching is halted adjacent to a pn junction when a potential is applied across it. Another process uses a combination of laser milling and anisotropic etching to form triangular cross section resonators.[51] The laser machining is used to form parallel trenches in the <110> silicon which are then exposed to an anisotropic etchant that undercuts the middle region forming a triangular beam.

Surface micromachining[52-54] processes form resonators on the surface of the wafer. This is usually achieved using sacrificial layer technology.[55] This approach involves depositing and patterning two films on top of each other on the wafer surface. The top film will form the resonator whilst the bottom film is the sacrificial layer which is selectively etched leaving the resonator raised above the substrate. The thin films used for each layer and the etchant type must be

carefully chosen to ensure that only the sacrificial layer is etched, and care must also be taken to protect the substrate from the etchant.

The advantages of surface micromachining include its compatibility with IC processes and small resonator size thereby increasing the number of devices per unit area of wafer. Disadvantages include variation in the deposited film's material properties, the residual stresses often present in the films and the inherent fragility of such small structures. However a number of devices have recently been demonstrated.[19,54,56,57]

For quartz or GaAs the fabrication processes are not as well developed as for silicon. Quartz is the most restricted due to the lack of any known etch stop mechanism. Wet and dry etching processes exist and for z-cut quartz wafers the high degree of anisotropy enables thick structures to be machined with near vertical side walls.[58] The fabrication of GaAs resonators can be achieved using processes that are similar to those available for silicon.[59] Selective etch stop techniques, sacrificial layer technologies, wet and dry anisotropic etching and high strength bonding processes are all available, though to date these processes are more expensive and not as well characterised as the equivalent silicon process.

6: Cross Sensitivities

6.1 Temperature and time

The causes of a resonator's temperature coefficient of frequency have been discussed elsewhere.[1,43] In summary the temperature coefficient is controlled by the vibration mode, the resonator material and any stresses induced by differential thermal expansion of packaging or deposited layers on the resonator.

Resonators tend to have very stable frequencies with time. The following factors have been identified which may effect the stability of resonant frequency assuming environmental effects are kept constant.

6.1.1 Relief of packaging or fabrication stress

Stress may be built into a microengineered resonator during its fabrication, for example by boron doping, the deposition of passivating SiO_2 layers over detection piezoresistors, or the fabrication of vacuum sealing caps. It can also be introduced when mounting the sensor chip for example by bonding on a pyrex header at high temperature or by epoxy mounting on an alumina substrate. Such stresses will relieve with time and repeated temperature cycling resulting in frequency drift.

6.1.2 Bias sensitivities

Electrostatic drive of a resonator requires that the ac sinusoidal drive waveform be superimposed on a DC bias. This ensures that the driving force's frequency is the same as the ac sinusoidal drive frequency (rather than double it as occurs if no bias is present). The DC bias affects the resonant frequency causing an offset in the resonator's frequency.[56] The offset will vary should the DC voltage reference vary. Similar effects exist with other drive techniques.[57]

Detection techniques also produce similar problems. For example, resistive thermal drive causes localised resonator heating resulting in frequency changes as a result of stress and temperature rises. The value of these stresses will change as, in this case, the resistors drift thus causing unwanted frequency drift.

6.1.3 Changes in material properties with time

This effect will be small when compared with factor 6.1.1. It results from diffusion of impurities or changes in the crystal structure due to imperfections in the crystal lattice.

7: Conclusions

The high performance of resonant sensors coupled with the low cost of micromachined resonators promises significant market penetration for resonant microsensors.

To date micromachined resonant devices are commercially available for absolute and differential pressure measurement and rotation rate. Resonant accelerometers have also been demonstrated in the past.

8 : References

1 G. Stemme: J. Micromech Microeng **1** (1991) 113.

2 R. Langdon: J Phys E: Sci Instrum **18** (1985) 103.

3 Paper 4 in this special issue.

4 J.C. Greenwood: J Phys E: Sci. Instrum **17** (1984) 650.

5 K.Petersen, S. Pourahmadi, J. Brown, P. Parsons, M. Skinner and M. Tudor: Proc. Transducers '91, California, USA (1991) pp 664.

6 C.J. Welham, J.W. Gardner and J. Greenwood: Proc. 8th Int. Conf. on Solid-State Sensors and Actuators (Transducers '95) and Eurosensors IX, Stockholm, Sweden (1995) p. 586.

7 D.W. Satchell and J.C. Greenwood: Sensors and Actuators **A24** (1989) 241.

8 D.W. Burns, R.D. Horning, W.R. Herb, J.D. Zook and H. Guckel: : Proc. 8th Int. Conf. on Solid-State Sensors and Actuators (Transducers '95) and Eurosensors IX, Stockholm, Sweden (1995) p. 659.

9 Chr. Burrer and J. Esteve: Sensors and Actuators **A50** (1995) 7.

10 C. Lu and A.W. Czanderna: Application of piezoelectric quartz crystal microbalances (Elsevier, Amsterdam, 1984).

11 E. Stemme and G. Stemme: IEEE Trans Electron Devices **37** No 3 (1990) 648.

12 R. Blevins: Formulus for natural frequancy and mode shape (Robert E. Krieger Publishing Co. Inc.,1979) Chap. 8.

13 M. Hashimoto, C. Cabuz, K. Minami and M. Esashi: J. Micromech. Microeng. **5** (1995) 219.

14 K. Tanaka, Y. Mochida, M. Sugimoto, K. Moriya, T. Hasegawa, K. Atsuchi and K. Ohwada: Sensors and Actuators **A50** (1995) 115.

15 Y. Li and P. Lapp: Petroleum Refinary **32** (1953) 119.

16 V.M. Mecea: Sensors and Actuators **A40** (1994) 1.

17 M.K. Andrews, G.C. Turner, P.D. Harris and I.M. Harris: Sensors and Actuators **A36** (1993) 219.

18 O. Paul, O. Brand and H. Baltes: J. Vac. Sci. Technol. **A13(3)** (1995) 503.

19 K. Ikeda, H. Kuwayama, T. Kobayashi, T. Watanabe, T. Nishikawa and T. Yoshida: Tech Digest 7th Sensor Symp, (1988), 55.

20 S. C. Chang, M.W. Putty, D.B. Hicks and C.H. Li: Sensors and Actuators **A21-A23** (1990) 342.

21 J. Söderkvist: Sensors and Actuators **A43** (1994) 65.

22 S.P. Beeby and M.J. Tudor: J. Micromech. Microeng. **5** (1995) 103.

23 H.A.C. Tilmans and S Bouwstra: Workshop Digest Micro Mechanics Europe MME'93, Neuchatel, Switzerland, September 1993, p. 138.

24 R.A. Buser and N.F. DeRooij: Sensors and Actuators **A21-A23** (1990), 323.

25 R.T. Howe: IEEE Trans Electron Devices **ED-33** (1986), 499.

26 J. Söderkvist: IEEE Trans Ultrasonics, Feroelectrics and Frequency Control, **Vol 38(2)** (1991) 271.

27 H. Guckel, C. Rypstat, M. Nesnidal, J.D. Zook, D.W. Burns and D.K. Arch: Tech Digest IEEE Sol St Sensor and Actuator Workshop, 22-25th June 1992, 153.

28 J. Söderkvist and K. Hjort: Sensors and Actuators A **39** (1993) 133.

29 T. Fabula, H.J. Wagner and B. Schmidt: Sensors and Actuators **41-42** (1994) 375.

30 H.A.C. Tilmans: Micromechanical sensors using encapsulated built in strain gauges, PhD thesis, University of Twente, The Netherlands, 1993.

31 A.B. Pippard: The Physics of Vibration Vol 1, (Cambridge University Press, 1978).

32 J.G.Eisly: J Appl Mathematics and Physics **15** (1964) 167.

33 K. Ikeda, H. Kuwayama, T. Kobayashi, T. Watanabe, T. Nishikawa, T. Yoshida and K. Harada: Sensors and Actuators **A21-23** (1990) 146.

34 M.V. Andres, K.W.H. Foulds and M.J Tudor: Electron Lett **23(18)** (1987) 952.

35 H.J. Pain: The Physics of Vibrations and Waves, (John Wiley & Son 4th Ed. 1993).

36 J.P. Den Hartog: Mechanical Vibrations (McGraw Hil, 1940) p186.

37 J.C. Greenwood and T. Wray: Sensors and Actuators **A37-A38** (1993), 82.

38 Silicon sensors and microstructures, (1988), Pub. Lucas Novasensor, 1055 Mission Court, Fremont, CA 94539, California, USA.

39 H. Offereins, H. Sandmaier, B. Folkmer, U. Stager, W. Lang: Proc Microsystems Technology '90, Berlin, 515.

40 S. Spiering, S. Bouwstra, R. Spiering: Sensors and Actuators **A39** (1993) 149.

41 M.A. Schmidt and R.T. Howe: Ceram. Eng. Sci, Proc. **8** (1987) 1014.

42 K.E. Petersen: Proc. IEEE **70** (1982), 420.

43 M.J. Tudor, M.V. Andres, K.W.H. Foulds and J.M. Naden: Proc. IEEE **135** (1988) 364.

44 T.I. Kamins: Sensors and Actuators **A21-A23** (1990) 817.

45 H. Guckel, J.J. Sniegowski, T.R. Christenson and F. Raissi: Sensors and Actuators **A21-23** (1990) 345.

46 E.P. Eernisse, R.W. Ward and R.B. Wiggins: IEEE Trans UFFC **Vol. 35** No. 3 (1988) 323.

47 B. Hok and K. Gustafsson: Sensors and Actuators **8** (1985) 235.

48 S. Beeby: Mechanical Isolation of Miniature Resonant Transducers and Stress Relieving Packages, PhD Transfer Thesis, USITT, Southampon University, England.

49 H. Holloway and S. McCarthy: J Appl Phys **73** (1993) 103.

50 R. Huster, A. Kovacs and A. Stoffel: MME 1993 Workshop Digest, 79.

51 M. Alavi, T. Fabula, A. Schumacher and H. Wagner: Sensors and Actuators, **37-38** (1993) 661.

52 C. Linder, L. Paratte, M.A. Grétillat, V.P. Jaecklin and N.F. DeRooij: J Micromech Microeng **2** (1992) 122.

53 H. Guckel: Sensors and Actuators A28 (1991) pp 133.

54 R.T. Howe and R.S. Muller: IEEE Trans Elec. Dev. ED-33 No. 4 (1986) pp 499.

55 C. Linder and N.F. de Rooij: Sensors and Actuators **A21-23** (1990) pp 1053.

56 H.A.C. Tilmans and R. Legtenburg: Sensors and Actuators **A45** (1994) 67.

57 H.A.C. Tilmans, M. Elwenspoek and J.H.J. Fluitman: Sensors and Actuators, **A38** (1992) 35.

58 L.D. Clayton, E.P. Eernisse, R.W. Ward and R.B. Wiggins: Sensors and Actuators **A20** (1989) pp 171.

59 J. Miao, J. Würfl, K. Fricke, D. Rück and H.L. Hartnagel: Micro Mechanics '93 Workshop Digest, Sept. 1993, Neuchatel, Switzerland, pp 51.

Name / Reference	Function	Structure	Matl.	Process	Drive	Mode	Freq (kHz)	Q (*1000)
Greenwood [4]	Pressure	Butterfly	Si (p++)	BMM	Electro-static	T	70	10.00
Howe [25]	Vapour	Bridge	Poly-Si	SMM	E¬ lectr o-static	F	270.00	-
Ikeda et al [19]	Pressure	H Shape	Si (p++)	BMM	Magnetic	F	30	50.00
Satchell and Greenwood [7]	Accelera-tion	TBTF	Si	BMM	Thermal (resistor)	F	65.00	2.70
Buser and De Rooij [24]	Pressure	Plate	Si	BMM	Electro-static	T	24.00	600.00
Söderkvist [26]	Gyro	TF	Quartz	BMM	Piezo-electric	F	37.00	13.7*
Guckel et al [27]	Pressure	Bridge	Poly-Si	SMM	Electro-static	F	568.00	47.00
Stemme and Stemme [11]	Pressure	Diaphragm	Si	BMM + SFB	Electro-static	F	14.10	2.6*
Söderkvist and Hjört [28]	Test	TF	GaAs	BMM	Piezo-electric	T	33.00	27*
Fabula et al [29]	Force	TBTF	Si/ZnO	BMM	Piezo-electric	F	17.60	0.40
Tilmans [30]	Strain gauge	Bridge	Poly-Si	SMM	Electro-static	F	323.70	0.60
Andrews et al [17]	Pressure	Plate	Si	BMM	Electro-static	F	20	20-30 (0.01-0.02)*
Burns et al [8]	Accelera-tion	Bridge	Poly-Si	SMM+ BMM	Electro-static	F	500	20

Table I - Example resonant sensors
(BMM - Bulk micromachined, SMM - Surface micromachined,
T - Torsional, F - Flexural, * at atmospheric pressure)

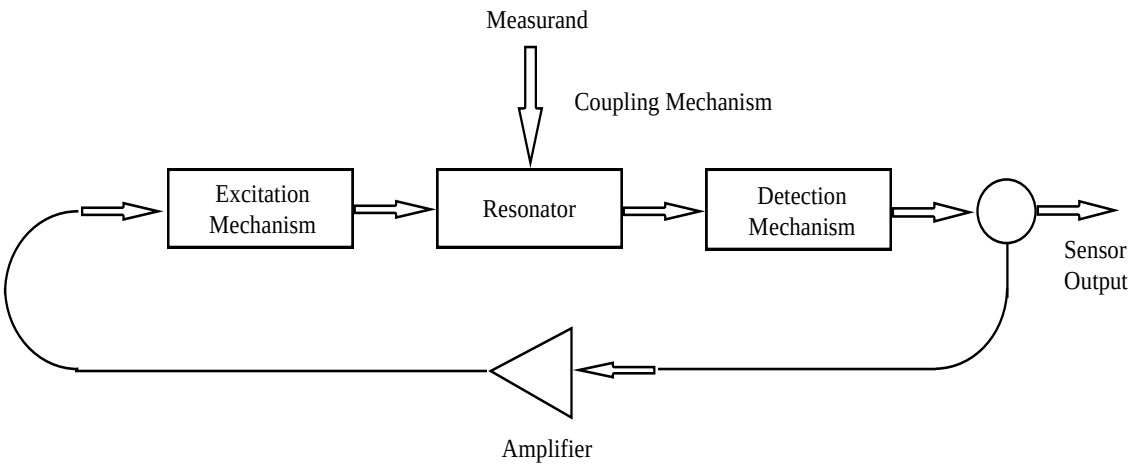

Fig. 1. Block diagram of a resonant sensor.

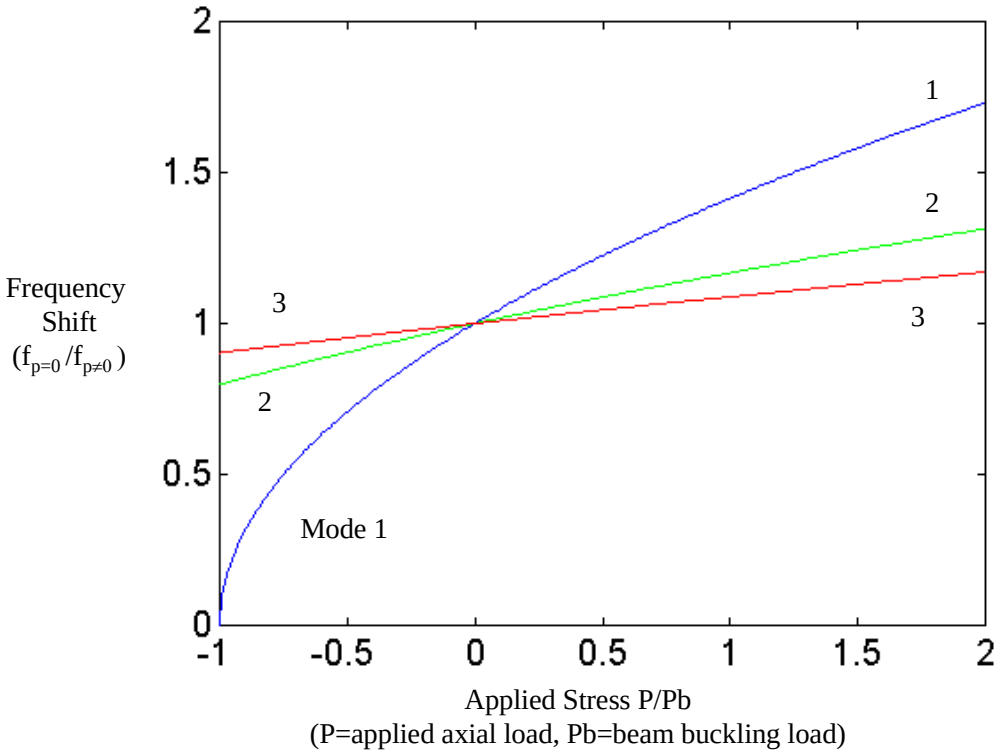

Fig. 2. Stiffness induced frequency change.

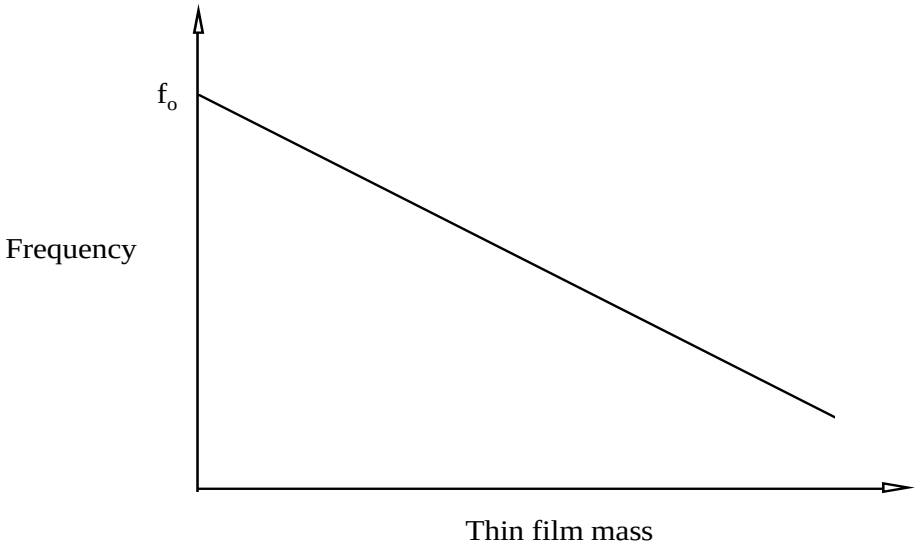

Fig. 3. Added-mass induced frequency change.

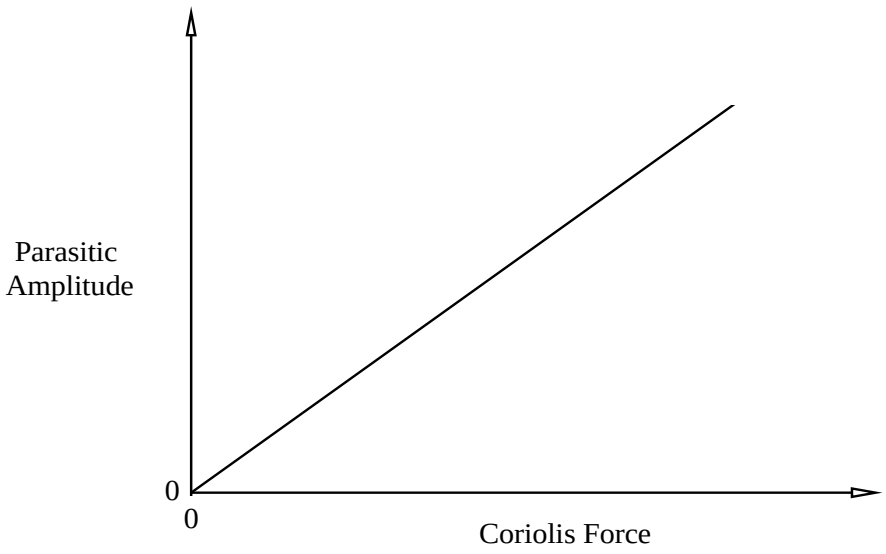

Fig. 4. Corriolis force induced parasitic vibration

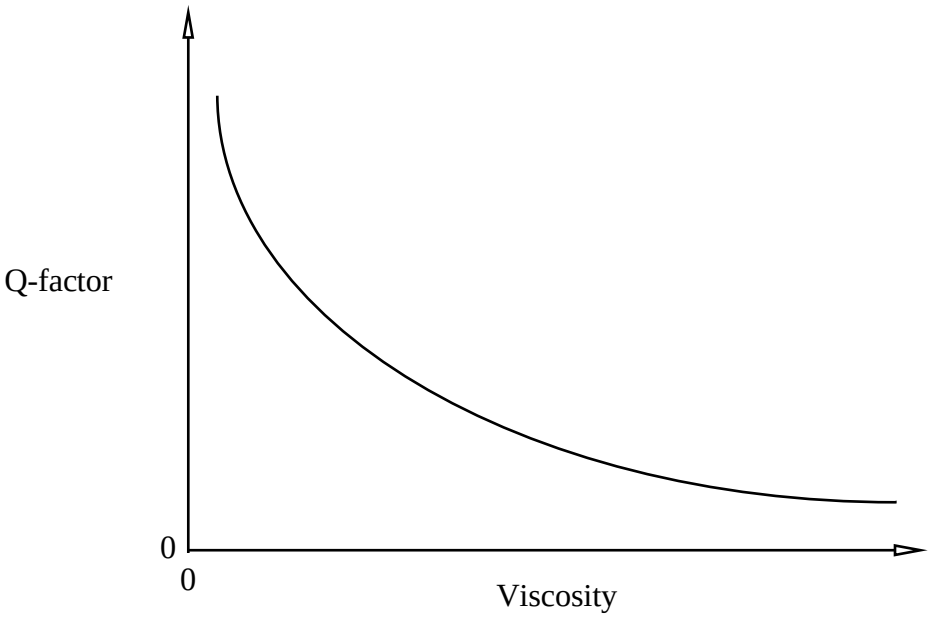

Fig. 5. Q factor as a function of the viscosity of the surrounding fluid

Figure 5: A micromachined resonant silicon pressure sensor (Acknowledgement is made to Druck Ltd for permission to publish)

Figure 6: A micromachined resonant silicon accelerometer (Acknowledgement is made to BNR Europe for permission to publish)